Complexation of Poly(vinyl alcohol)–Congo Red Aqueous Solutions. 1. Viscosity Behavior and Gelation Mechanism

Mitsuhiro Shibayama,* Fumiyoshi Ikkai, Ryuji Moriwaki, and Shunji Nomura

Department of Polymer Science and Engineering, Kyoto Institute of Technology, Matsugasaki, Sakyo-ku, Kyoto 606, Japan

Received August 16, 1993; Revised Manuscript Received January 3, 1994®

ABSTRACT: The complexation of poly(vinyl alcohol) (PVA) with congo red (CR) ions in aqueous solutions was investigated as functions of PVA (C_{PVA}) and congo red concentrations (C_{CR}) and temperature. The PVA–CR complexation resulted in a gelation around pH 7 when both C_{PVA} and C_{CR} were high enough. However, in the case of intermediate PVA concentrations in monomer unit, i.e., 0.6 mol/L, a sol–gel–sol–gel-type transition was observed with increasing CR concentration. The origin of this "re-entrant"-type phase transition was studied by estimation of the enthalpy of cross-link formation and by capillary viscometry. The gelation was classified into two steps: (a) weak cross-link and (b) strong cross-link formations. These mechanisms were characterized by the value of the enthalpy of cross-link, ΔH. The former is in the order of −5 kcal/mol and the latter −20 kcal/mol. This viscosity behaviors in a dilute polymer concentration regime were also classified into several regions: When both C_{CR} and C_{PVA} were low, the complex solution showed a typical viscosity behavior for a polyelectrolyte solution. With increasing C_{CR} and C_{PVA}, there appeared a region where a time-dependent viscosity thickening took place. With further increase in C_{PVA}, the viscosity recovered a behavior similar to that for a PVA solution without CR. The connection between these rheological properties and sol–gel transition is discussed by taking into account the ionic screening effect and complexation equilibria.

1. Introduction

Poly(vinyl alcohol) (PVA) aqueous solutions undergo gelation due to a complexation with several ions, such as borate,[1] cupric,[2] titanate,[3] and vanadate ions.[4] These kinds of gels are sensitive to pH, and a sol–gel transition is usually observed by changing pH. This is due to the fact that the ionization equilibrium of these ions is controlled by pH, which leads to a drastic change of the concentration of "cross-linkers". Another unique feature of PVA is that it is capable of hydrogen bonding itself, which plays an important role in the crystallization of PVA as well as the gelation. We have been investigating the mechanisms of PVA gelation in aqueous solutions, such as PVA–borate gels[5,6] and PVA–vanadate gels.[7] However, these gels have to be prepared in strong basic (PVA–borate gels) or strong acidic conditions (PVA–vanadate gels), which constrains the application of these gels.

Congo red (CR), the first synthesized direct dye, has also been known as a viscosity thickening reagent and/or gelation reagent for PVA aqueous solutions.[8] The chemical structure of congo red (CR) is shown in Figure 1a. A direct dye, which means that it can be used to color object materials without the addition of any other reagent, generally has the following properties:[19] (1) rather linear and plain molecular architecture; (2) the presence of functional groups capable of hydrogen bonding, such as azo and amino groups; (3) high ionization in an aqueous solution due to the presence of sulfate groups; and (4) ease in self-association in an aqueous solution, as shown in Figure 1b, for example. Therefore, CR can be regarded as a suitable candidate for a complexation reagent to study PVA–ion complexation at neutral or mild basic conditions.

It is expected that an attached charge in a PVA–CR complex (monocomplex) can be easily dissociated by changing the ionic environment, resulting in a drastic change in the rheological properties of the polymer solution. On the other hand, if the attached charge is coupled with another polymer segment (i.e., dicomplexation), a cross-link is formed, which leads to a clustering, phase demixing, and/or gelation of the polymer solution. Thus, these polymer–ion complexes provide a variety of aspects of rheological properties as well as the state of the polymer solution. As a matter of fact, a novel sol–gel transition behavior, a sol–gel–sol–gel transition, is exclusively found in PVA–CR complex solutions, as is shown in Figure 2. The objective of this paper is to elucidate the origin of this interesting sol–gel transition behavior of PVA–CR ion complexes in aqueous solutions in terms of the results of gelation thermodynamics and viscosity measurements for these complexes. In a forthcoming

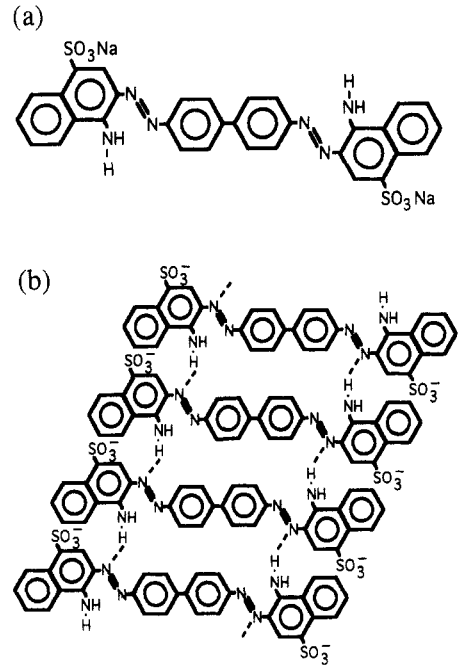

Figure 1. Chemical structure of congo red molecule (a) and a proposed structure of congo red aggregates (b).

* Author to whom correspondence should be addressed.

® Abstract published in *Advance ACS Abstracts*, February 15, 1994.

0024-9297/94/2227-1738$04.50/0

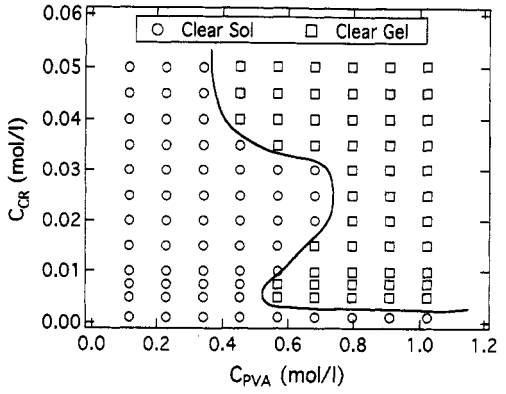

Figure 2. Phase diagram showing the sol–gel transition of PVA–CR complexes in aqueous solutions aged for 120 h at 20 °C.

paper,[10] we will report the microscopic view of the sol–gel transition of PVA–CR complexes studied with small-angle neutron and X-ray scattering techniques.

2. Experimental Section

2.1. Sample. Poly(vinyl alcohol) in powder form having the viscosity-average degree of polymerization P of about 1800 was supplied by Nippon Synthetic Chemical Industry Co., Ltd. The degree of saponification was 99.96 mol %. The diad tacticity was determined by ^{13}C NMR to be 27.8% syndio, 50.2% hetero, and 22.2% isotactic. The polydispersity of PVA was measured by GPC on the acetylated polymer, i.e., poly(vinyl acetate). The ratio of the weight- and number-average molecular weights, M_w/M_n, was 2.34. PVA aqueous solutions were prepared by dissolving the PVA powder in deionized water at 80 °C. Congo red (CR) of purified grade, purchased from Nakarai Tesque Co. Ltd., was also dissolved in deionized water with stirring. The prescribed PVA and CR solutions were mixed at 80 °C and kept in a temperature-controlled room at 20 °C. Some of the PVA–CR solutions gradually became a gel. It was found that aging for 120 h was long enough to evaluate the equilibrium state of the complex.

2.2. Phase Diagram and Sol–Gel Transition Temperature Measurement. The state of each sample was simply examined with a tilting-a-test-tube method. When the sample solution did not flow by turning the test tube containing the sample upside down, we decided that the solution was gelled. The sol–gel transition temperature, T_{gel}, was measured by the same method described above during the course of temperature scanning with the rate of $^1/_{15}$ °C/min.

2.3. Viscosity Measurements. The viscosity of PVA–CR complex solutions was measured with a Ubbelohde capillary viscometer at 60 ± 0.05 °C. The time required for the solution to pass the two meniscuses of the Ubbelohde capillary viscometer was recorded. A typical time was in the order of 100 s and was very reproducible with an error of ±0.1 s, in most of the cases. Thus, the relative error in the relative viscosity of the solution to that of the solvent was estimated to be about 0.1%.

3. Results and Discussion

3.1. Phase Diagram. Figure 2 shows the phase diagram of PVA–CR complexes at 20 °C aged for 120 h after sample preparation. The abscissa and ordinate are the PVA (C_{PVA}) and congo red concentrations (C_{CR}), respectively. The open circles and open squares indicate sols and gels, respectively. The solid curve denotes the sol–gel transition curve. Both sols and gels were clear and red in all of the concentration regions, and no turbidity was observed. Although the complex is in a sol state for the low cross-linker (CR) and polymer (PVA) concentration regime and in a gel state for the high concentration regime, the sol–gel transition curve has an interesting behavior around C_{PVA} = 0.57 mol/L and C_{CR} = 0.025 mol/L. This means that there appears a sol–gel–sol–gel transition by increasing

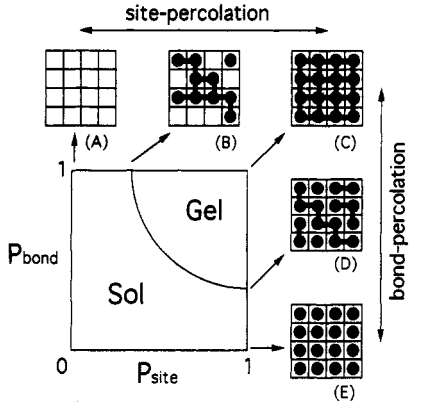

Figure 3. Schematic representation of the site-bond percolation model. P_{site} and P_{bond} denote the site and bond probabilities, respectively. Solid circles and tie lines in (A)–(E) indicate the site (monomer) and bonds, respectively.

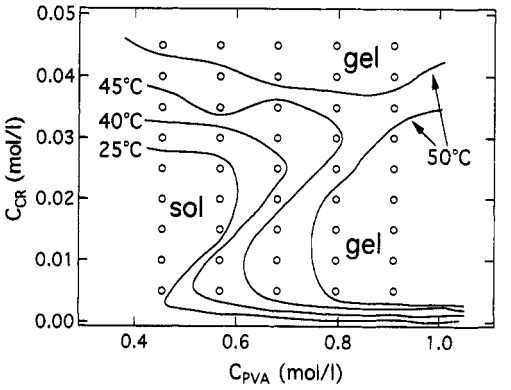

Figure 4. Temperature variation of the gel–sol transition curve. Open circles in the figure denote the sampling points.

the cross-linker concentration, C_{CR}, for C_{PVA} = 0.57 and 0.68 mol/L.

Generally, a sol–gel transition behavior of polymer solutions can be well described with a site-bond percolation model[11,12] as schematically depicted in Figure 3. The phase, sol or gel, is governed by two parameters, i.e., the bond probability, P_{bond}, and the site probability, P_{site}. If P_{bond} = 1, the sol–gel transition is dependent on the fraction of sites occupied by monomers (indicated by closed circles), which is P_{site}. The infinite cluster is formed for case B in the figure. On the other hand, if P_{site} = 1, the gelation is determined by P_{bond} as shown in (C–E). In the case of PVA–borate complex in an aqueous solution, the sol–gel transition was well described by the site–bond percolation model as was studied elsewhere,[5,6] where the borate concentration and C_{PVA} were corresponding to P_{bond} and P_{site}, respectively. However, this is not the case for the PVA–CR complex. We call this sol–gel–sol–gel transition, observed exclusively in PVA–CR, a "re-entrant" sol–gel transition.

Figure 4 shows the contour map of the states of PVA–CR at several temperatures. The open circles in the figure indicate the set of concentrations (C_{PVA}, C_{CR}) at which the sol–gel behavior was examined. It is now clear that there exist two types of gels discriminated by C_{CR}. With increasing temperature, the sol region intrudes into the gel region. At 50 °C the gel region is clearly separated into two domains. Note that these gels are completely dissolved at 60 °C.

3.2. Enthalpy of Gel Melting. Figure 5 shows the gel–sol transition (gel melting) temperatures for gels having several C_{CR}'s as a function of C_{PVA}. Although T_{gel} increases with C_{PVA}, the slope seems to depend on C_{CR}. Gels of C_{CR} > 0.03 mol/L have less dependence of T_{gel} on C_{PVA} than

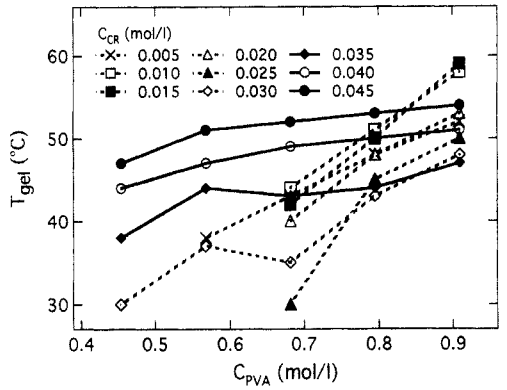

Figure 5. C_{PVA} dependence of the gel–sol transition temperature, T_{gel}. Dashed and solids lines indicate low and high C_{CR} regions, respectively.

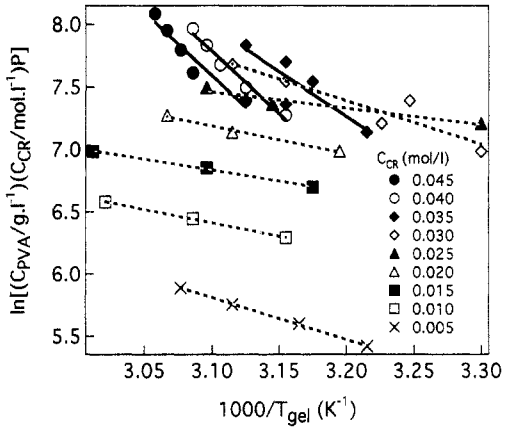

Figure 6. ln ($C_{PVA}PC_{CR}$) vs $1/T_{gel}$ plots for gel melting of PVA–CR complexes. Dashed and solid lines, the least-squares fits of the data points, indicate the low and high C_{CR} regions, respectively.

others. The origin of the C_{CR} dependence of T_{gel} can be elucidated by evaluating the enthalpy of gel melting, ΔH, as will be discussed in the following.

According to the modified Eldridge–Ferry theory of gel melting,[5] the polymer concentration at gel melting (C_{gel}) is related to the cross-linker concentration, i.e., C_{CR}, and the degree of polymerization (P), and is given by

$$\ln (C_{gel}PC_{CR}) = \text{constant} + \frac{\Delta H}{RT_{gel}} + \ln \frac{[H^+] + K_I}{K_I} \quad (1)$$

where ΔH and K_I are, respectively, the enthalpy of cross-link formation and the ionization constant of CR. R, T_{gel}, and $[H^+]$ are the gas constant, the gel–sol transition temperature, and the proton concentration, respectively. As for PVA–CR complexes, the ionization of CR is on the order of 10^{-4} mol/L. Therefore, at the neutral condition, i.e., pH ≅7, most CR molecules are ionized. Therefore, $[H^+]$ is much lower than K_I in most of the cases in our study. Thus, eq 1 is rewritten as

$$\ln (C_{gel}PC_{CR}) = \text{constant} + \frac{\Delta H}{RT_{gel}} \quad (2)$$

Figure 6 shows the plots of ln ($C_{PVA}PC_{CR}$) vs $1/T_{gel}$. It is clearly recognized that the slopes are varying with C_{CR}. Particularly, high C_{CR}'s, discriminated with solid lines, have larger magnitudes of ΔH.

Figure 7 shows C_{CR} dependence of the enthalpy of cross-link formation which is calculated with eq 2. ΔH increases with C_{CR} for $C_{CR} \leq 0.020$ mol/L and has a broad maximum around $C_{CR} = 0.020$ mol/L. Then ΔH decreases with C_{CR}

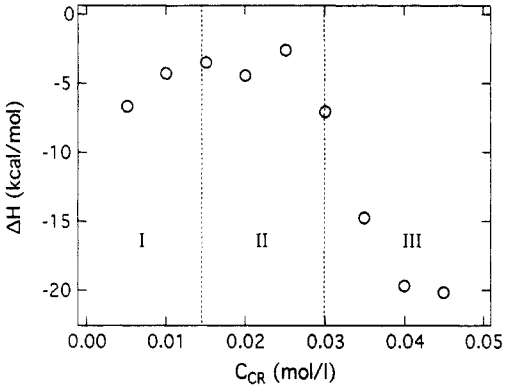

Figure 7. C_{PVA} dependence of the enthalpy of cross-link formation, ΔH. The variation of ΔH is divided into three regimes, denoted I–III.

and reaches about −20 kcal/mol. The minus sign means that the gelation is an exothermic process. Since the variation of ΔH corresponds to the phase behavior in Figure 2, it is reasonable to classify the C_{CR} dependence of ΔH into three regimes: (I) the weak gelation regime with $\Delta H \leq -5$ kcal/mol for $C_{CR} < 0.015$ mol/L; (II) the dissociation regime with $\Delta H \geq -5$ kcal/mol for 0.015 mol/L $< C_{CR} <$ 0.03 mol/L; and (III) the strong gelation regime with $\Delta H \leq -15$ kcal/mol for $C_{CR} > 0.03$ mol/L. Note that C_{CR}'s for the dissociation regime correspond to the sol phase between the two gel phases in Figures 2 and 4.

3.3. Electrostatic Screening Effect on Gelation. In the previous section, it was found that two types of PVA–CR gels were present depending mostly on C_{CR}. Note that in the case of PVA–borate complexes, the observed ΔH was almost invariant with respect to the cross-linker concentration.[5] In this section, we clarify the essential difference between these gels. Knowing that PVA–borate gels require a basic environment, we usually add NaOH of the order of 10^{-1} mol/L to ensure a full ionization of boric acid. This means that the concentrations of hydroxyl ions, $[OH^-]$, and sodium ions, $[Na^+]$ are on the order of 10^{-1} mol/L. Therefore, it is easily expected that the nature of the polyelectrolyte is greatly suppressed for the case of the PVA–borate complex since the Debye screening length, r_D, is about 7 Å for the borate concentration, $C_{borate} = 0.01$ mol/L.[13] On the other hand, that for the PVA–CR complex is about 18 Å, which results in a polyelectrolyte-type behavior where a strong repulsive electrostatic interaction appears. This leads to an intrachain cross-linking rather than an interchain cross-linking formation. We guess that this intrachain cross-link results in gel melting in the intermediate C_{CR}'s. When C_{CR} is low, CR molecules effectively take part in a gelation via interchain cross-links. However, with increasing C_{CR}, PVA chains favor intrachain cross-links to gain the translational entropy by gel melting, which occurs in regime II. With further increase in C_{CR}, excess CR molecules may behave as salt ions which screen the repulsive interaction between the tagged CR molecules on PVA chains. Thus, the PVA–CR complex recovers a gel state. This speculation was examined by studying the phase behavior of PVA–CR complexes in the presence of a large amount of added salt.

Figure 8 shows the phase diagram of PVA–CR complexes in an aqueous solution. The samples and the experimental conditions are exactly the same as in the case of Figure 2, except that 0.095 mol/L of NaOH was added to the solution. The anomalous behavior, seen in Figure 2, is not observed, and a simple sol–gel transition curve is recovered here. This sol–gel transition behavior is quantitatively similar to that of the PVA–borate ion complex.[6]

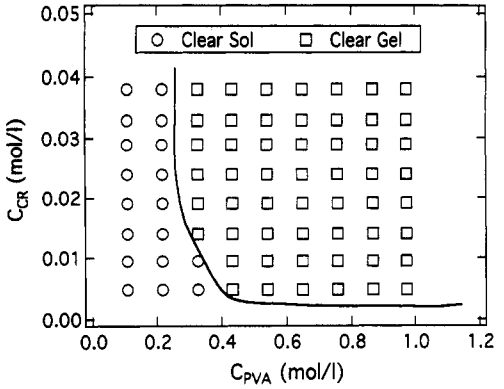

Figure 8. Phase diagram showing the sol–gel transition of PVA–CR complexes at a high basic condition, [NaOH] = 0.095 mol/L.

In other words, the concentrations of the polymer and the cross-linker at the sol–gel transition are almost the same in the two cases even though the cross-linker is different. These facts clearly indicate that the unique behavior seen in the PVA–CR complex around the intermediate concentration regime is due to a polyelectrolyte behavior of PVA–CR complexes.

3.4. Viscosity. We conducted viscosity measurements in a dilute polymer solution regime so as to obtain more evidence about the polyelectrolyte behavior and electrostatic screening effect in PVA–CR complexes. We begin with the discussion of the chain overlap concentration in monomeric units, C_{PVA}*, where the PVA chains in a solution start to overlap each other.

C_{PVA}* is roughly estimated by

$$C_{PVA}^* = 3Pm/4\pi N_A R_g^3 \quad (3)$$

where m is the monomer molecular weight, N_A is Avogadro's number, and R_g is the radius of gyration. For an unperturbed PVA chain having the degree of polymerization P, R_g can be estimated by

$$R_g = \frac{b_{PVA}}{\sqrt{6}} P^{1/2} \quad (4)$$

where b_{PVA} is the statistical segment length of the PVA chain. By using the value of b_{PVA} = 6.3 Å,[14] one gets C_{PVA}* = 0.55 mol/L for a PVA having P = 1800 in a theta solvent. Note that C_{PVA}* = 0.45 mol/L was estimated for the PVA–vanadate ion complexes having P = 1700.[7] In the case of the PVA–vanadate ion complexes, η_R increases or decreases with time depending on C_{PVA}. The increase is due to interchain cross-linking and the decrease to intrachain cross-linking. The concentration at which η_R became invariant with respect to time corresponds to C_{PVA}*. C_{PVA}* for the PVA–vanadate ion complex was thus estimated.

a. Congo Red Concentration Dependence. Figure 9 shows η_R vs C_{CR} plots for PVA–CR solutions having several C_{PVA} values. Although these C_{PVA} values are smaller than the calculated C_{PVA}*, we should bear in mind that we are examining the crossover region from dilute to semidilute regimes because of the fact that PVA chains are expected to be highly expanded owing to the attached ions. η_R shows an upturn at high C_{CR}. This is due to a finite cluster formation of PVA cross-linked by CR. The C_{CR} value, where η_R shows the upturn, increases with C_{PVA}, indicating that the cluster formation is suppressed by increasing C_{PVA} at a given C_{CR} (>0.03 mol/L). This result contradicts our expectations. For instance, the site-bond percolation model, discussed in Figure 3, predicts that the higher the polymer concentration or cross-linker concentration, the lower the gelation concentration.[11,12] Therefore, the upturn, which is regarded as a preliminary phenomenon of gelation, should shift to lower concentration with increasing C_{PVA}. This contradiction will be solved by introducing the concept of the electrostatic screening effect, which will be discussed in detail in section 3.5.

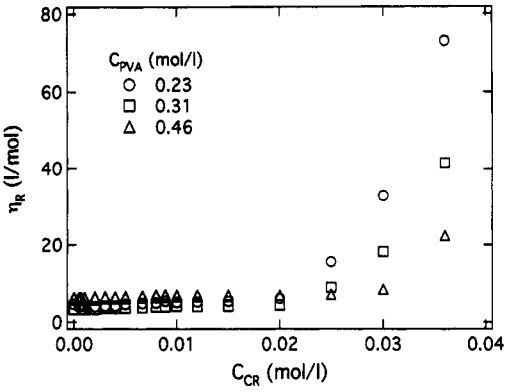

Figure 9. CR concentration, C_{CR}, dependence of η_R for several PVA concentrations, C_{PVA} = 0.23, 0.31, and 0.46 mol/L.

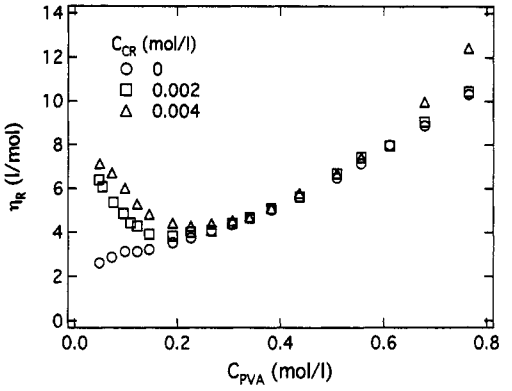

Figure 10. PVA concentration, C_{PVA}, dependence of η_R without and with CR (C_{CR} = 0.002 and 0.004 mol/L).

b. PVA Concentration Dependence. Figure 10 shows the C_{PVA} dependence of η_R for low C_{CR} values. In the case of C_{PVA} = 0, η_R behaves just as expected for a neutral polymer solution. When CR is added, η_R shows an upturn at low C_{PVA}, typical for polyelectrolytes. The higher C_{CR}, the higher η_R at low C_{PVA}. This clearly indicates that CR ions attached to PVA chains repel each other, resulting in increase in the chain size. This kind of polyelectrolyte effect was not observed for PVA–borate complexes, as shown in Figure 3 of ref 6. However, when C_{CR} was further increased, more surprising results were obtained, as shown in Figure 11.

Figure 11 shows the variation of η_R as a function of C_{PVA} for various CR concentrations. η_R starts to show a distinct maximum with increasing C_{CR} at the intermediate concentration range of PVA, 0.05 < C_{PVA} < 0.4 mol/L. A viscosity thickening was observed exclusively in this concentration regime. The plots shown here correspond to the equilibrium values of η_R, which were measured 4 days after installation of the solution into a viscometer. For C_{PVA} > 0.4 mol/L, however, η_R becomes insensitive to C_{CR} as well as time, and the viscosity varies similarly to that for the PVA aqueous solution, i.e., C_{CR} = 0. The maximum value of η_R is about 10–100 times as high as that for the case with C_{CR} = 0 compared at the same C_{PVA}. Another interesting observation is that the C_{PVA}, where η_R recovers the behavior of the noncharged PVA solution, is roughly proportional to C_{CR}.

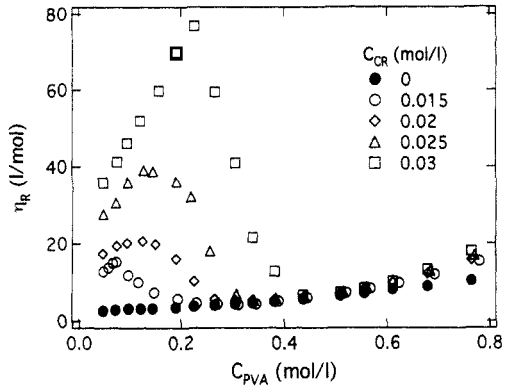

Figure 11. C_{PVA} dependence of η_R without and with CR. Note that the concentration range of C_{CR} is taken much larger than those in Figure 10.

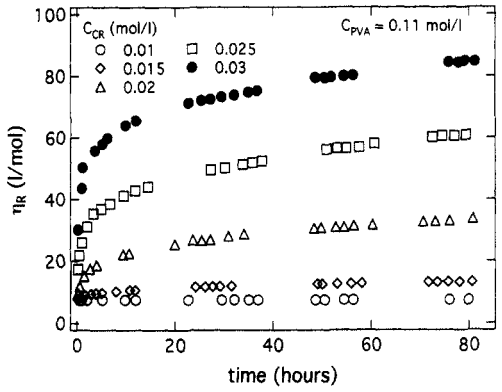

Figure 12. Time dependence of η_R for PVA–CR complexes having different CR concentrations.

c. Time Evolution of the Reduced Viscosity. The reduced viscosity of PVA–CR complex solutions was time dependent in the limited regime, where a peak appeard in Figure 11, i.e., the regime for $C_{CR} > 0.015$ mol/L and $0.05 < C_{PVA} < 0.4$ mol/L. No time evolution in η_R was observed for $C_{CR} < 0.01$ mol/L or $C_{PVA} > 0.4$ mol/L. Figure 12 shows the time evolution of η_R for PVA–CR complexes having several C_{CR} values. It takes roughly 4 days to reach an equilibrium in η_R for all of the samples having different C_{CR} values. Note that each data point was taken on a freshly prepared PVA–CR solution aged for a given period of time. The change in η_R with time seems to be more distinct for PVA–CR complexes having higher C_{CR} values.

3.5. Explanation of the Viscosity Behavior with C_{PVA}. First of all, we explain the viscosity behavior shown in Figure 11 in a qualitative manner by using the schematic pictures in the upper part of Figure 13. The lower figure is a reproduction of η_R vs C_{PVA} plots for the cases of C_{CR} = 0.025 mol/L and C_{CR} = 0 mol/L in Figure 11. It is convenient to classify the behavior of η_R to four regimes, I–IV, as shown in the figure. It should be noted here that the relative CR concentration with respect to C_{PVA} is inversely proportional to C_{PVA} and that the roles of CR ions are of (1) cross-linkers, (2) added salt, and (3) ions attached to PVA chains depending on the relative concentration of CR with respect to PVA.

In regime I, each PVA chain is highly attached by CR ions and is surrounded by a large number of free CR ions. The large number of free CR ions shields repulsive electrostatic interaction and promotes cluster formation of PVA chains via dicomplexation between monocomplexes and free PVA chains. The cluster size increases with C_{PVA}, resulting in the increase in η_R with C_{PVA}. However, by further increase in C_{PVA}, the relative C_{CR} decreases and the repulsive interaction becomes strong.

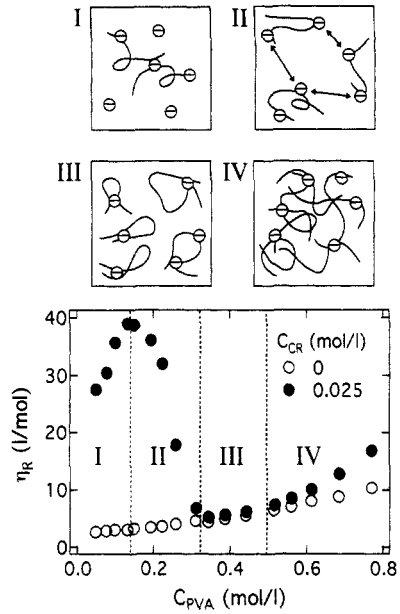

Figure 13. Schematic pictures for the conformation of PVA–CR complexes (upper) and the variation of η_R as a function of C_{PVA} (lower). Arrows in scheme II indicate strong electrostatic repulsion between attached charges.

In this concentration regime, PVA clusters dissociate into individual chains with a large number of attached CR ions. Thus, PVA chains behave as polyelectrolytes in a solution, of which η_R decreases C_{PVA}. This is regime II. In regime III, where PVA chains are entangled, strong repulsive electrostatic interaction is depressed due to the excluded volume effect of PVA chains. CR ions lead to intrachain cross-linking to gain the translational entropy of PVA chains. This results in a contraction of the chain size, and thus η_R becomes roughly identical to that for the PVA solutions without CR. In regime IV, where the C_{PVA} is much higher than the chain overlap concentration, C_{PVA}^*, the major contributor to η_R is chain entanglements. However, in the case of the PVA–CR complexes, the presence of intermolecular cross-links provides an additional increase in the viscosity as a symptom of gelation. Thus, the difference in η_R again appears.

It should be marked here that CR ions are molecularly dispersed in an aqueous solution when the temperature is high enough, e.g., 60 °C. This was confirmed by ^{1}H NMR of CR deuterated water solution.[13] It is definite, on the other hand, that a large number of CR clusters exist at the temperature of observation. However, these clusters act as free ions rather than cross-linkers since PVA–CR solutions were prepared at 80 °C, at which only nonclustered CR ions are intercalated among PVA chains. Schemes I–IV in Figure 13 are depicted taking account of this fact.

3.6. Gelation Mechanism. On the basis of the results of gelation thermodynamics and viscosity measurements discussed above, we propose a gelation mechanism of PVA–CR complexes. Figure 14 schematically shows the gelation mechanism of PVA–CR complexes. The solid curves and the open ovals which surround a minus sign indicate PVA chains and CR ions, respectively. First, for a low C_{CR}, CR molecules effectively act as cross-link points. Second, in the intermediate C_{CR} regime, the electrostatic repulsion between CR molecules on PVA chains leads to a gel melting. At high C_{CR}, on the other hand, the excess free CR ions shield the electrostatic interaction between attached CR ions, recovering a cross-link formation.

The variation in ΔH may indicate an additional mechanism of gel formation. Provided the gelation mechanism

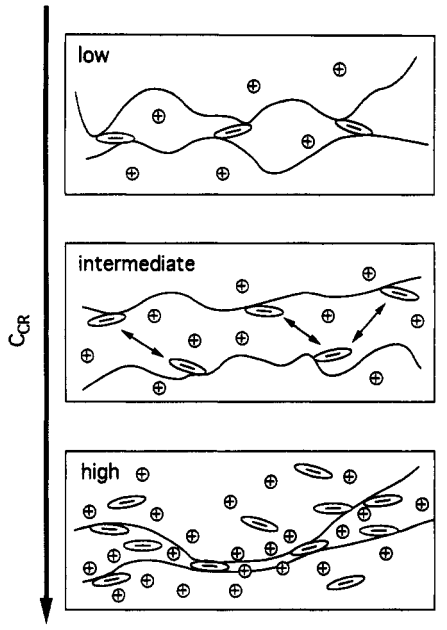

Figure 14. Schematic diagram showing cross-link formation of PVA (solid curves) with CR ions (ovals with minus signs). The counterions are denoted by circles with plus signs.

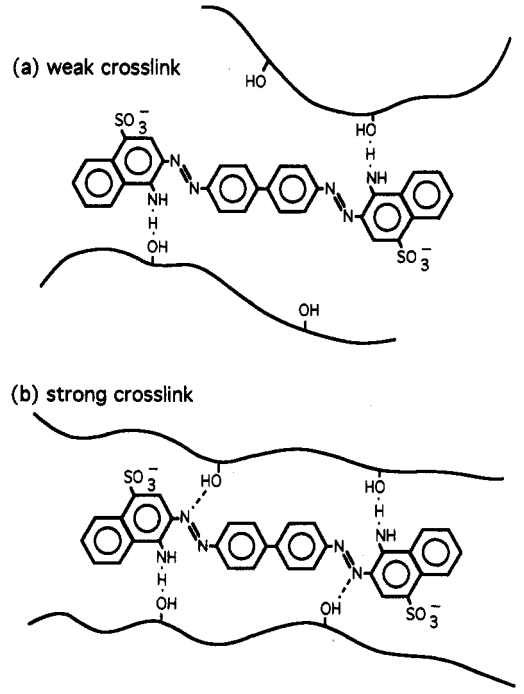

Figure 15. Schematic representation of the cross-link structures of PVA complexes.

is the same, ΔH should be a constant since it is defined as an enthalpy of cross-link formation. However, the observed ΔH varied from −5 to −20 kcal/mol, clearly indicating that the gelation mechanism changes according to C_{CR}. Figure 15 shows tentative models for the structures of (a) a weak cross-link and (b) a strong cross-link. As shown here, the additional cross-link formation may take place via azo nitrogens. Another aspect for the strong cross-link may be a successive formation of hydrogen bonding along the PVA chains[7,15,16] since PVA molecules themselves have a capability of hydrogen bonding if two PVA molecules are at least locally aligned in parallel. A PVA–CR cross-link could be even a nucleus for hydrogen-bonded PVA crystallites, which also act as a physical cross-link. Some of these strong cross-link formation mechanisms stabilize the cross-link structure with time and increase the magnitude of the enthalpy of gel melting by 4 times from −5 to −20 kcal/mol. The two types of gelation mechanisms can be symbolized by "point cross-link" (a) and "line cross-link" (b), since a series of cross-links are formed along PVA chains like a zipper[17] in the case of the strong cross-link.

Further analysis of the structure of PVA–CR complexes by small-angle X-ray and neutron scattering is discussed elsewhere.[10]

4. Conclusions

The gelation mechanism of PVA–CR complexes in aqueous solutions was studied. The following facts were disclosed: (1) A gelation occurs around pH 7, and the sol–gel transition temperature depends on both C_{PVA} and C_{CR}. (2) A re-entrant sol–gel phase transition was observed for intermediate concentrations of PVA and CR. This characteristic behavior is observed only in the absence of added salt. (3) There are two types of gels characterized by the enthalpy of cross-link formation, and those correspond to weak and strong cross-links depending on the ionic environment. (4) The reduced viscosity, η_R, behavior for low C_{CR} is very similar to those for polyelectrolyte solutions without salt. However, for a high C_{CR} regime, η_R, has a distinct maximum and the maximum becomes higher with increasing C_{CR}. (5) In the range where η_R has a maximum, a time evolution of η_R was also detected. The time required to attain an equilibrium was on the order of a few days. This time evolution in η_R was explained with a successive formation of hydrogen bonds.

On the basis of these findings, the re-entrant sol–gel transition, found exclusively in PVA–CR complex aqueous solutions, was successfully interpreted in the light of polyelectrolyte nature and complexation equilibria of PVA chains and CR ions.

Acknowledgment. We thank Prof. Kanji Kajiwara, Department of Materials Engineering, Kyoto Institute of Technology, and Prof. Y. Rabin, Bar-Ilan University, Israel, for fruitful discussion. This work is supported by the Ministry of Education, Science and Culture, Japan (Grants-in-Aid 04805092 and 05805080 to M.S.).

References and Notes

(1) Deuel, H.; Neukom, A. *Makromol. Chem.* **1949**, *3*, 113.
(2) Saito, S.; Okuyama, H. *Kolloid Z.* **1954**, *139*, 150.
(3) Crisp, J. D. U.S. Pat. 258193, 1946.
(4) Kawakami, H.; Fujiwara, H.; Kinoshita, Y. Jpn. Pat. S47-40894, 1972.
(5) Shibayama, M.; Yoshizawa, H.; Kurokawa, H.; Fujiwara, H.; Nomura, S. *Polymer* **1988**, *29*, 20667.
(6) Kurokawa, H.; Shibayama, M.; Ishimaru, T.; Wu, W.; Nomura, S. *Polymer* **1992**, *33*, 2182.
(7) Shibayama, M.; Adachi, M.; Ikkai, F.; Kurokawa, H.; Sakurai, S.; Nomura, S. *Macromolecules* **1993**, *26*, 623.
(8) Fujino, K.; Fujimoto, N. *Sen-i Gakkaishi* **1959**, *15*, 483.
(9) Vickerstaff, T. *The Physical Chemistry of Dyeing*, 2nd ed.; Oliver and Boyd: London, 1954.
(10) Shibayama, M.; Ikkai, F.; Nomura, S. *Macromolecules* (submitted for publication).
(11) Coniglio, A.; Stanley, H. E.; Klein, W. *Phys. Rev. Lett.* **1979**, *42*, 518.
(12) Stauffer, D. *Introduction to Percolation Theory*; Taylor & Francis: London, 1985.
(13) Ikkai, F.; Shibayama, M.; Moriwaki, R.; Nomura, S. Unpublished results.
(14) Shibayama, M.; Kurokawa, H.; Nomura, S.; Roy, S.; Stein, R. S.; Wu, W. *Macromolecules* **1990**, *23*, 1438.
(15) Wu, W.; Shibayama, M.; Roy, S. K.; Kurokawa, H.; Coyne, R. D.; Nomura, S.; Stein, R. S. *Macromolecules* **1990**, *23*, 2245.
(16) Shibayama, M.; Kurokawa, H.; Nomura, S.; Muthukumar, M.; Stein, R. S.; Roy, S. *Polymer* **1992**, *33*, 2883.
(17) Ilmain, F.; Tanaka, T.; Kokufuta, E. *Nature* **1991**, *349*, 400.